Full optical phonon spectrum and Fröhlich Hamiltonian in wurtzite-type free-standing quantum well wires

D. E. N. Brancus* and L. Ion†
Faculty of Physics, University of Bucharest, Strasse Atomistilor nr. 405, P.O. Box MG-11, 077125 Magurele-Ilfov, Romania
(Received 8 May 2007; revised manuscript received 10 September 2007; published 5 October 2007)

In the context of the dielectric-continuum model used here for a uniaxial crystal, the dispersion laws of the full optical phonon spectrum of a quantum wire made of a wurtzite-type material and the corresponding Fröhlich electron-phonon interaction terms are obtained. The coupling function describing the electron-phonon interaction is obtained in an analytical closed form, which depends, mainly on the dispersion law of the phonon branch involved. The Fröhlich Hamiltonian for the full optical phonon spectrum is obtained based on the general orthogonality relation proven for the eigenvectors of the phonon field. Numerical calculations are performed for ZnO and GaN quantum wires. In the frame of Rayleigh-Schrödinger perturbation theory, the polaron problem is discussed in a GaN quantum wire.

DOI: 10.1103/PhysRevB.76.155304 PACS number(s): 63.22.+m, 63.20.Kr, 68.65.La

I. INTRODUCTION

The general progress experienced in the past two decades by the semiconductor nanotechnology requires investigation on the electron-optical-phonon interaction in low-dimensional systems. In such systems, the electron-optical-phonon interaction is recognized for affecting several physical properties such as electron scattering rates, hot-electron energy losses, polaron effects, etc. This interaction, called Fröhlich interaction, has mainly been investigated by using the dielectric continuum (DC) model.[1] The advantage of using the DC model is that it allows obtaining analytical closed-form expressions. In addition, the results obtained with the DC model are in good agreement with those resulting from detailed microscopic calculations[2–4] and found in experiments.[5,6]

Initially, the electron-optical-phonon interaction has been examined in low-dimensional systems, such as quasi-two-dimensional (q-2D) heterostructures, quantum wires (QWRs), and quantum dots (QDs), made of optically isotropic semiconductor materials. However, in the past years, anisotropic materials, such as ZnO, GaN, AlN, and InN, have became of great interest due to their prospective applications in electronics.[7–9] Thus, by using the DC model, the properties of the optical phonons and their interaction with the conduction electron in q-2D anisotropic uniaxial structures, such as double heterostructures (isotrop/anisotrop/isotrop),[10] wurtzite-type heterostructures with single and double heterointerfaces,[11] single quantum wells,[12] infinite superlattices,[13] and arbitrary wurtzite multilayer heterostructures,[14,15] have been theoretically investigated. Also, the same interesting problem of the optical phonons in the interaction with electrons has been investigated in anisotropic GaN/AlN QDs.[16–18] An experimental study[19] of Raman scattering in GaN/AlN QDs was reported, too.

Recently, a new low-dimensional anisotropic semiconductor system, that of QWR, came into attention, both experimentally[20–26] and theoretically.[27–29] However, with the exception of the classification[27,28] of other possible types of optical phonon modes, the theoretical studies were devoted only to the interface phonon modes and their interaction with electrons in wurtzite AlN/GaN/AlN cylindrical QWR,[27] GaN/AlN QWR,[28] and multishell wurtzite cylindrical QWs.[29]

It is the aim of this paper to discuss, based on the DC model, the full spectrum of the optical phonons, including the quasilongitudinal and quasitransverse modes and their interaction with electrons in a wurtzite cylindrical free-standing QWR. The coupling function, describing the interaction between the conduction electrons and the different phonons (quasilongitudinal, quasitransverse, and surface), will be obtained in analytical form, determined by their corresponding phonon dispersion law. Consequently, the Fröhlich Hamiltonian including the contributions of all types of optical phonons is found, allowing us to discuss the polaron problem in such anisotropic systems.

The paper is organized as follows. In Sec. II, we introduce the dielectric-continuum model appropriate for our considered low-dimensional anisotropic system. In Sec. III, we present the properties of all types of phonon modes obtained from the corresponding three-dimensional (3D) extraordinary phonon modes. The general orthogonality relation for eigenvectors of the phonon field used in Sec. III is explicitly derived in Appendix A. In Sec. IV, the Hamiltonian of the interaction between the optical phonon modes and a conduction electron is obtained. Numerical results for ZnO and GaN are shown in both Secs. II and III. In Sec. V, we discuss the polaron problem in an anisotropic QWR with numerical application only for GaN.

II. EQUATIONS OF THE MODEL

We consider an anisotropic uniaxial (cylindrical) wire of radius R with the optical axis directed along the axis of the wire. The optical phonon field is discussed in the context of the Born-Huang model, which is generally known as the dielectric-continuum model. For the sake of simplicity, we will limit ourselves to the case of such polar crystals for which the optical phonon field can be described by a 3D real vector. This assumption, yielding a dielectric function with two-oscillator contributions, allows us to discuss the dynamics of the optical phonons in uniaxial crystals such as

wurtzite-type materials (CdS, ZnO, GaN, and AlN), layered materials (InSe, GaSe, PbI_2, SnS_2, etc.), and other polar materials. However, numerical results presented in the following sections are restrained to the particular case of some wurtzite-type materials (ZnO and GaN).

By denoting the optical phonon field, the electric field, and the polarization field by the vectors $\vec{u}(\vec{r},t)$, $\vec{E}(\vec{r},t)$, and $\vec{P}(\vec{r},t)$, the equations of the model are[30]

$$\ddot{\vec{u}}_\alpha(\vec{r},t) = \beta_{11}^\alpha \vec{u}_\alpha(\vec{r},t) + \beta_{12}^\alpha \vec{E}_\alpha(\vec{r},t),$$

$$\vec{P}_\alpha(\vec{r},t) = \beta_{12}^\alpha \vec{u}_\alpha(\vec{r},t) + \beta_{22}^\alpha \vec{E}_\alpha(\vec{r},t), \tag{1}$$

where $\alpha = \parallel$ and $\perp$; the symbols $\parallel$ and $\perp$ correspond to a direction that is either parallel or orthogonal to the optical axis. The β coefficients have the expressions[31]

$$\beta_{11}^\alpha = (\omega_{TO}^\alpha),$$

$$\beta_{12}^\alpha = \varepsilon^{1/2}[\varepsilon_\alpha(0) - \varepsilon_\alpha(\infty)]^{1/2}\omega_{TO}^\alpha,$$

$$\beta_{22}^\alpha = \varepsilon_0[\varepsilon_\alpha(\infty) - 1], \tag{2}$$

where $\varepsilon_\alpha(0)$, $\varepsilon_\alpha(\infty)$, and ω_{TO}^α are the low frequency dielectric constant, the high frequency dielectric constant, and the transverse phonon mode frequency, respectively. All quantities are considered along the principal direction α; ε_0 is the vacuum permittivity.

By taking into account Eqs. (1) and the forms of β coefficients, the components of the dielectric tensor are obtained as

$$\varepsilon_\alpha(\omega) = \varepsilon_\alpha(\infty)\frac{(\omega_{LO}^\alpha)^2 - \omega^2}{(\omega_{TO}^\alpha)^2 - \omega^2}, \tag{3}$$

ω_{LO}^α being the longitudinal phonon mode frequency along the principal direction α.

We shall discuss the problem in the context of the electrostatic approximation. The form of the electrostatic potential, including also the contribution of surface charges, is

$$\Phi(\vec{r},t) = -\frac{1}{4\pi\varepsilon_0}\int_V dv' \nabla_{\vec{r}}\left(\frac{1}{|\vec{r}-\vec{r}'|}\right)\vec{P}(\vec{r}',t). \tag{4}$$

For 2D anisotropic systems, it has been shown[10,31] that it is more convenient to work with the components of the phonon field rather than those of the polarization field. This is because, unlike the eigenvectors of the polarization field, the eigenvectors of the phonon field corresponding to different frequencies are orthogonal. The same approach will be used later for our quasi-one-dimensional (q-1D) anisotropic system.

In the following, by using Eq. (4) together with the equations of the dielectric-continuum model, a system of integral equations will be obtained for the components of the phonon field. First, the polarization field is written in terms of partial Fourier transforms:

$$\vec{P}_\alpha(\vec{r},t) = \varepsilon_0 g_\alpha(\omega)\chi_\alpha(\omega)\vec{u}_\alpha(\vec{r},\omega), \tag{5}$$

where $\chi_\alpha(\omega)$ is the α component of the dielectric susceptibility tensor and

$$g_\alpha(\omega) = [(\omega_{TO}^\alpha)^2 - \omega^2]/\beta_{12}^\alpha. \tag{6}$$

By choosing the x_3 axis along the optical axis, the following system of integral equations is obtained for the Cartesian components of the optical phonon field:

$$g_i(\omega)u_i(\vec{r},\omega) = \frac{1}{4\pi}\frac{\partial}{\partial x_i}\int_V dv' \nabla_{\vec{r}}\left(\frac{1}{|\vec{r}-\vec{r}'|}\right)\vec{G}(\vec{r}',\omega), \tag{7}$$

where the following notations are introduced: $i=1$, 2, and 3; $g_1(\omega)=g_2(\omega)=g_\perp(\omega)$; $g_3(\omega)=g_\parallel(\omega)$; and

$$\vec{G}(\vec{r},\omega) = g_\parallel(\omega)\chi_\parallel(\omega)\vec{u}_\parallel(\vec{r},\omega) + g_\perp(\omega)\chi_\perp(\omega)\vec{u}_\perp(\vec{r},\omega). \tag{8}$$

According to the electrostatic approximation

$$\nabla \times \vec{E} = 0, \tag{9}$$

Eq. (7) leads to

$$\nabla \times [g_\parallel(\omega)\vec{u}_\parallel(\vec{r},\omega) + g_\perp(\omega)\vec{u}_\perp(\vec{r},\omega)] = 0. \tag{10}$$

It is worth mentioning that the same result can be obtained directly from Eq. (1) by observing that the combination inside the parentheses is just the expression of the electric field intensity $\vec{E}$.

Furthermore, the divergence of the vector $\Sigma_{\alpha=\perp,\parallel} g_\alpha(\omega)\vec{u}_\alpha(\vec{r},\omega)$ can be constructed from the left side of Eq. (7), obtaining

$$g_\parallel(\omega)\varepsilon_\parallel(\omega)\,\nabla\,\vec{u}_\parallel(\vec{r},\omega) + g_\perp(\omega)\varepsilon_\perp(\omega)\,\nabla\,\vec{u}_\perp(\vec{r},\omega) = 0. \tag{11}$$

Then, by combining Eqs. (10) and (11), the classical differential equation for the electrostatic potential Φ inside the wire is obtained

$$\varepsilon_\parallel(\omega)\frac{\partial^2\Phi}{\partial x_3^2} + \varepsilon_\perp(\omega)\left(\frac{\partial^2\Phi}{\partial x_1^2} + \frac{\partial^2\Phi}{\partial x_2^2}\right) = 0. \tag{12}$$

Outside the wire, the electrostatic potential obeys Laplace's equation:

$$\Delta\Phi = 0. \tag{13}$$

In the following, rather than searching for the solutions of integral Eq. (7), we choose to solve the problem of the phonon field by using the differential equations (12) and (13), and the relationship between the electrostatic potential and the phonon field:

$$g_\parallel(\omega)\vec{u}_\parallel(\vec{r},\omega) + g_\perp(\omega)\vec{u}_\perp(\vec{r},\omega) = -\nabla\Phi. \tag{14}$$

To do that, we have to consider first the standard electrostatic boundary conditions at the surface of the cylindrical wire:

(a) the continuity of the electrostatic potential at the surface of the system

$$\Phi_{in}|_\Sigma = \Phi_{out}|_\Sigma; \tag{15}$$

(b) the continuity of the normal component of the dielectric displacement vector

$$\vec{n}\cdot\vec{D}_{in}|_{\Sigma}=\vec{n}\cdot\vec{D}_{out}|_{\Sigma}; \tag{16}$$

$\vec{n}$ being the unit vector parallel to the exterior normal of the cylindrical surface.

The solution of Eq. (12) can be written in a compact form in cylindrical coordinates:

$$\Phi_{in}(\rho,z,\varphi)=\sum_{m,q}A_{mq}W_{mq}(z,\varphi)F_{mq}(\rho). \tag{17}$$

By considering periodic boundary conditions along the optical axis of the system, we obtain

$$W_{mq}(z,\varphi)=\frac{1}{\sqrt{2\pi L}}e^{iqz}e^{im\varphi}, \tag{18}$$

where L is the length of the wire, q takes the values determined by the cyclic boundary conditions $\left(q_r=\frac{2\pi r}{L}, r=0,\pm1,\pm2,\ldots\right)$, and m has the values $0,\pm1,\pm2,\ldots$.

Depending on the behavior of the functions $\varepsilon_{\parallel}(\omega)$ and $\varepsilon_{\perp}(\omega)$, the specific forms of the function $F_{mq}(\rho)$ are

(a) for $s(\omega)=\frac{\varepsilon_{\perp}(\omega)}{\varepsilon_{\parallel}(\omega)}>0$,

$$F_{mq}(\rho)=I_{|m|}\left(\frac{|q|\rho}{\sqrt{s}}\right), \tag{19}$$

where $I_{|m|}(x)$ is the modified Bessel function of the first kind;

(b) for $s(\omega)<0$,

$$F_{mq}(\rho)=J_{|m|}\left(\frac{|q|\rho}{\sqrt{|s|}}\right), \tag{20}$$

where $J_{|m|}(x)$ is the Bessel function of the first kind. Outside the wire, the electrostatic potential has the expression

$$\Phi_{out}(\rho,z,\varphi)=\sum_{mq}B_{mq}W_{mq}(z,\varphi)K_m(|q|\rho), \tag{21}$$

$K_m(x)$ being the modified Bessel function of the second kind.

III. OPTICAL PHONON MODES

The dispersion laws of the phonon modes in an anisotropic uniaxial wire will be obtained in the following by using forms (17) and (21) of the electrostatic potential inside and outside the wire and considering the boundary conditions (15) and (16). By knowing the electrostatic potential, the components of the eingenmodes of the phonon field can then be calculated from Eq. (14).

According to the different types of solutions for $F_{mq}(\rho)$, the optical phonon modes can be classified as surface phonon modes and confined phonon modes (quasilongitudinal and quasitransverse). In the following, we shall introduce a new index μ with the values $\mu=0$ for the surface phonon modes, $\mu=1$ for the quasitransverse-phonon modes, and $\mu=2$ for the quasilongitudinal-phonon modes.

A. Surface phonon modes

The frequency range of these modes is determined by values for which the condition discussed above at (a) is fully satisfied. Dispersion laws of these modes are given by the relation

$$f_{mq}^{(0)}=0, \tag{22}$$

where

$$f_{mq}^{(0)}=\frac{\varepsilon_{\perp}(\omega)}{\sqrt{s(\omega)}}-\frac{I_{|m|}\left(\frac{|q|R}{\sqrt{s}}\right)K_m'(|q|R)}{I_{|m|}'\left(\frac{|q|R}{\sqrt{s}}\right)K_m(|q|R)}, \tag{23}$$

with the inequality $\varepsilon_{\perp}(\omega)<0$ taken into account.

The spectrum is formed by a set of surface phonon branches having different indices m and depending on $|q|$. There is a degeneracy of these branches depending on the sign of m.

By using the trihedron for cylindrical coordinates with the unit vectors $\vec{e}_{\rho}$, $\vec{e}_{\varphi}$, and $\vec{e}_z$, the expressions of the components of the normal mode $(m,q,0)$ are

$$\vec{u}_{mq,\parallel}^{(0)}(\vec{r},\omega_{mq}^{(0)})=C_{mq}^{(0)}\frac{iq}{g_{\parallel}(\omega_{mq}^{(0)})}\vec{e}_z W_{mq}(z,\varphi)I_{|m|}\left(\frac{|q|\rho}{\sqrt{s}}\right), \tag{24}$$

$$\vec{u}_{mq,\perp}^{(0)}(\vec{r},\omega_{mq}^{(0)})=\frac{C_{mq}^{(0)}W_{mq}(z,\varphi)}{g_{\perp}(\omega_{mq}^{(0)})}\left[\vec{e}_{\rho}\frac{|q|}{\sqrt{s}}I_{|m|}'\left(\frac{|q|\rho}{\sqrt{s}}\right)+\vec{e}_{\varphi}\frac{im}{\rho}I_{|m|}\times\left(\frac{|q|\rho}{\sqrt{s}}\right)\right], \tag{25}$$

$C_{mq}^{(0)}$ being a normalization constant.

In Appendix B, after a cumbersome calculation, it is shown that the normalization constant can be put under the remarkable form

$$C_{mq}^{(0)}=\frac{\left(\frac{2\omega_{mq}^{(0)}}{\varepsilon_0|q|R}\right)^{1/2}}{\left|\left[I_{|m|}\left(\frac{|q|R}{\sqrt{s}}\right)I_{|m|}'\left(\frac{|q|R}{\sqrt{s}}\right)\frac{\partial f_{mq}^{(0)}}{\partial\omega}\right]_{\omega=\omega_{mq}^{(0)}}\right|^{1/2}}, \tag{26}$$

which represents a generalization to the anisotropic uniaxial case of the expression previously obtained for the isotropic material.[32]

B. Confined phonon modes

The confined phonon modes correspond to the solutions of the electrostatic potential obtained for $s(\omega)<0$. In the case of three-dimensional uniaxial crystals, these are the modes of the extraordinary optical phonons[1] which can be classified in quasilongitudinal modes and quasitransverse modes. For the particular case of wurtzite-type materials, there are two distinct frequency ranges, one of the quasilongitudinal phonon modes $[\varepsilon_{\perp}(\omega)<0$, i.e., $\omega\in(\omega_{LO}^{\parallel},\omega_{LO}^{\perp})]$ and one of the quasitransverse phonon modes $[\varepsilon_{\parallel}(\omega)<0$, i.e.,

$\omega \in (\omega_{TO}^{\parallel}, \omega_{TO}^{\perp})$]. The same situation is encountered in the case of uniaxial slab[31] and q-2D structures.[10,12] We shall keep the same classification also for the anisotropic uniaxial cylindrical quantum wire.

The dispersion laws of these confined phonon modes are obtained by solving the equation

$$f_{mq}^{(\mu)}(\omega) = 0, \quad \mu = 1 \text{ and } 2, \tag{27}$$

where

$$f_{mq}^{(\mu)}(\omega) = \frac{\varepsilon_{\perp}(\omega)}{\sqrt{|s(\omega)|}} - \frac{J_{|m|}\left(\frac{|q|R}{\sqrt{|s|}}\right)K'_m(|q|R)}{J'_{|m|}\left(\frac{|q|R}{\sqrt{|s|}}\right)K_m(|q|R)}. \tag{28}$$

For indices m, q, and μ fixed, a supplemental index l appears, labeling the different solutions of Eq. (27). In the case of isotropic materials,[32] this supplemental index l is associated with the lth zero of the Bessel function $J_{|m|}(x)$. At μ fixed, the spectrum is formed by a set of confined phonon branches, $\omega = \omega_{mql}^{(\mu)} = \omega_{ml}^{(\mu)}(q)$, depending on $|q|$ and having the indices m and l; the branches with the same $|m|$ are degenerated. Conventionally, we shall choose $\mu = 1$ for the quasitransverse modes and $\mu = 2$ for the quasilongitudinal modes.

The expressions of the components of the normal mode (m, q, l, μ; $\mu = 1$ and 2) are

$$\vec{u}_{mql,\parallel}^{(\mu)}(\vec{r}, \omega_{mql}^{(\mu)}) = \frac{iqC_{mql}^{(\mu)}}{g_{\parallel}(\omega_{mql}^{(\mu)})}\vec{e}_z W_{mq}(z,\varphi) J_{|m|}\left(\frac{|q|\rho}{\sqrt{|s|}}\right), \tag{29}$$

$$\vec{u}_{mql,\perp}^{(\mu)}(\vec{r}, \omega_{mql}^{(\mu)}) = \frac{C_{mql}^{(\mu)} W_{mq}(z,\varphi)}{g_{\perp}(\omega_{mql}^{(\mu)})}\left[\vec{e}_{\rho}\frac{|q|}{\sqrt{|s|}} J'_{|m|}\left(\frac{|q|\rho}{\sqrt{|s|}}\right) + \vec{e}_{\varphi}\frac{im}{\rho} J_{|m|} \times \left(\frac{|q|\rho}{\sqrt{|s|}}\right)\right]. \tag{30}$$

Following the procedure developed in Appendix B to obtain the normalization constant of the surface phonon modes, a compact expression is obtained for $C_{mql}^{(\mu)}$:

$$C_{mql}^{(\mu)} = \frac{\left(\frac{2\omega_{mql}^{(\mu)}}{\varepsilon_0 |q| R}\right)^{1/2}}{\left|\left[J_{|m|}\left(\frac{|q|R}{\sqrt{|s|}}\right) J'_{|m|}\left(\frac{|q|R}{\sqrt{|s|}}\right)\frac{\partial f_{mql}^{(\mu)}}{\partial \omega}\right]_{\omega=\omega_{mql}^{(\mu)}}\right|^{1/2}}. \tag{31}$$

In addition to the trivial orthogonality relation determined by the properties of the functions $W_{mq}(z,\varphi)$, based on the result of Appendix A and taking into account the phonon spectrum, the orthogonality of the eigenvectors of the optical phonon field is demonstrated:

$$\int_V dV \vec{u}_{mql}^{(\mu)*}(\vec{r}) \vec{u}_{m'q'l'}^{(\mu')}(\vec{r}) = \delta_{mm'}\delta_{qq'}\delta_{ll'}\delta_{\mu\mu'}. \tag{32}$$

We have to stress that following the line of calculation used in Appendix B is at hand to prove directly relation (32). In the particular case when we consider a surface mode and a confined mode, an extension of the Lommel integrals[33] by taking into account the pair $I_m(\lambda x)$ and $J_m(\mu x)$ needs to be derived.

In Figs. 1(a) and 1(b), the full spectrum of optical phonon modes is shown for ZnO and GaN. The following material parameters were considered: $\omega_{TO}^{\parallel} = 380$ cm^{-1}, $\omega_{TO}^{\perp} = 413$ cm^{-1}, $\omega_{LO}^{\parallel} = 579$ cm^{-1}, $\omega_{LO}^{\perp} = 591$ cm^{-1}, $\varepsilon_{\parallel}(\infty) = 3.78$, and $\varepsilon_{\perp}(\infty) = 3.70$ for ZnO,[34] and $\omega_{TO}^{\parallel} = 533$ cm^{-1}, $\omega_{TO}^{\perp} = 561$ cm^{-1}, $\omega_{LO}^{\parallel} = 735$ cm^{-1}, $\omega_{LO}^{\perp} = 743$ cm^{-1}, $\varepsilon_{\parallel}(\infty) = 5.29$, and $\varepsilon_{\perp}(\infty) = 5.29$ for GaN.[35] Regarding the quasilongitudinal modes, for both materials, the branches start from $\omega_{LO}^{\perp}$ for $|q|R \ll 1$ and go to $\omega_{LO}^{\parallel}$ at large values of $|q|R$. Here, the principal effect of the anisotropy is that of raising the strong degeneracy of the longitudinal-phonon spectrum as compared to the isotropic case where $\omega_{mql}^{(2)} = \omega_{LO}$. The behavior of the quasilongitudinal branches (m,l) is shown in the insets of both figures. In all the sections of the two figures, the phonon branches having the same value for m are drawn with the same type of line. The situation in our case is similar to that found in 3D or 2D uniaxial polar crystals and/or structures.

For $|m| \geqslant 1$, the branches of the surface modes start from $\omega = \omega_{TO}^{\perp}\sqrt{\frac{\varepsilon_{\perp}(0)+1}{\varepsilon_{\perp}(\infty)+1}}$, which is the solution of the equation $\varepsilon_{\perp}(\omega) = -1$, and for large values of $|q|R$ goes to the same value of frequency, which, in fact, is the only physically significant solution of the equation $\varepsilon_{\perp}(\omega)\varepsilon_{\parallel}(\omega) = 1$.

However, the behavior of the branch $\omega_0^{(0)}(q)$ is different. The limiting frequency $\omega_{TO}^{\perp}$ of the domain of frequencies of the surface modes is reached for a finite value q_0, according to the equation

$$\varepsilon_{\parallel}(\omega_{TO}^{\perp}) = \frac{2}{|q_0|R}\frac{K'_0(|q_0|R)}{K_0(|q_0|R)}. \tag{33}$$

The branch $\omega = \omega_0^{(0)}(q)$, which belongs to the surface modes, is defined for $|q| > |q_0|$. For large values of $|q|R$, this branch reaches the same value of frequency as the other surface-mode branches do. For smaller values of $|q|$ ($|q| < |q_0|$), the character of the surface-mode branch changes into that of quasitransverse-mode character, the branch $\omega = \omega_0^{(0)}(q)$ becoming the branch $\omega = \omega_0^{(1)}(q)$. This situation is observed for both considered materials. For $|q|R \gg 1$, the quasitransverse-phonon branches $\omega = \omega_m^{(1)}(q)$, $|m| \geqslant 1$, approach the limiting value $\omega_{TO}^{\perp}$. These unexpected result is a direct consequence of the distribution of the phonon frequencies $(\omega_{TO}^{\parallel}, \omega_{TO}^{\perp}, \omega_{LO}^{\parallel}, \omega_{LO}^{\perp})$, which is typical for wurtzite-type materials.

The situation is different for q-2D systems. Thus, for a uniaxial anisotropic slab[31] of wurtzite-type material, there is no such mode-character changing. However, for a material having a phonon-frequency distribution like $(\omega_{TO}^{\perp}, \omega_{TO}^{\parallel}, \omega_{LO}^{\perp}, \omega_{LO}^{\parallel})$, as in the case of PbI_2 slab,[31] two confined modes, one quasilongitudinal and one quasitransverse, become surface modes at different values of $|\vec{q}|$ (the modulus of in-plane wave vector). A similar situation is obtained in a

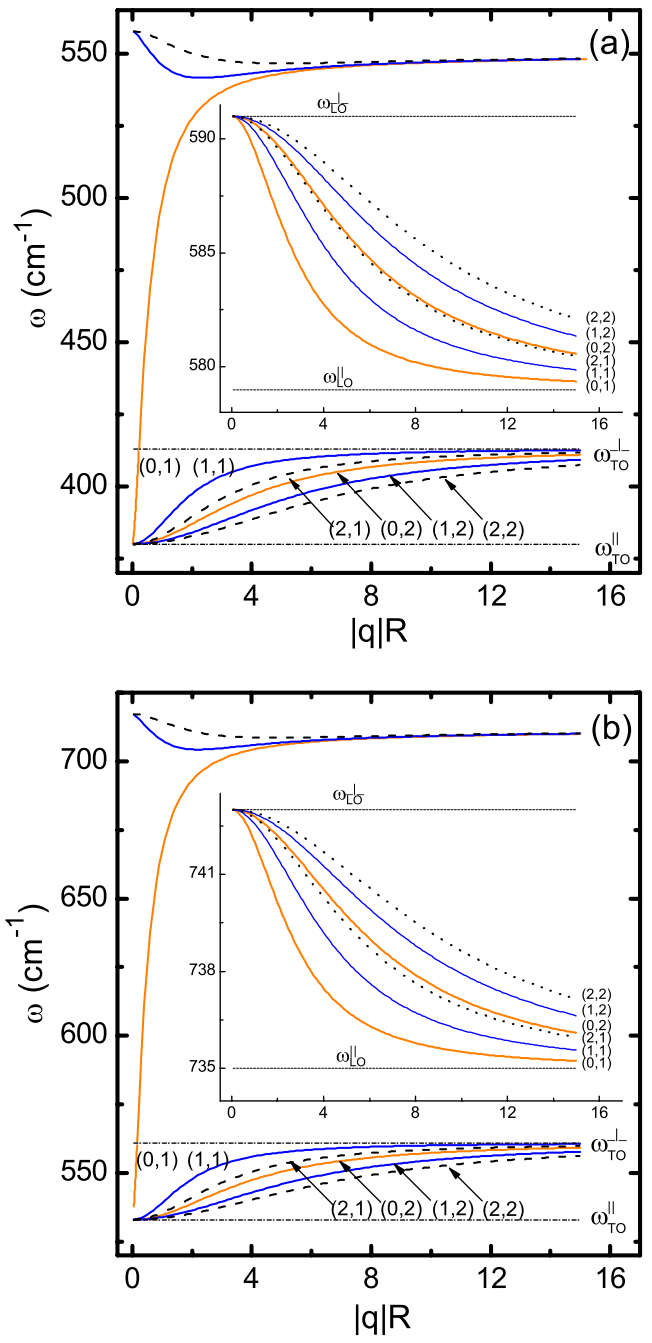

FIG. 1. (Color online) Optical phonon spectrum (a) for ZnO wire and (b) for GaN wire, respectively. The two quantum numbers (m,l) of each branch for the confined modes are indicated on the plot. The phonon branches of all types having the same value for m are drawn with the same type of line: orange (gray) solid line for $m=0$, blue (black) solid line for $m=1$, and black dashed line for $m=2$. In the inset, the behavior of the quasilongitudinal branches is presented; for clarity, $m=2$ phonon branches are drawn with a black dotted line here.

stressed GaAs/InP/GaAs (001) heterostructure,[36] in which case the distribution of the phonon frequencies $(\omega_{TO}^{\perp},\omega_{TO}^{\parallel},\omega_{LO}^{\perp},\omega_{LO}^{\parallel})$ of the uniaxially distorted InP material is realized.

IV. FREE PHONON HAMILTONIAN AND THE ELECTRON-PHONON INTERACTION

In this section, the Fröhlich Hamiltonian is obtained for an anisotropic QWR by paying equal consideration to all types of optical phonons. First, we will discuss the Hamiltonian of the free phonons. Zhang *et al.*[28] have obtained the Hamiltonian of the free optical phonons H_{ph} for the interface phonon modes only. Their approach was to start with a Hamiltonian density written in terms of the components of both fields, the phonon field and the local electric field $\vec{E}_{loc}$, and finally, to work with a Hamiltonian density depending on the components of the polarization field. Because the eigenvectors of the polarization field are not orthogonal in anisotropic systems, this approach is suitable for isotropic systems and anisotropic systems, but, in this latter case, when only one type of phonons needs to be considered. Here, in order to obtain the contributions of all types of phonons to H_{ph}, all the fields appearing in the form of the Hamiltonian density will be developed in terms of the eigenvectors of the phonon field, which verify the orthogonality relation (32). We choose to work with the following form of the Hamiltonian density:[37]

$$h_{ph}(\vec{r}) = \sum_{\alpha=\parallel,\perp} \frac{1}{2}[\Pi_{\alpha}^{2}(\vec{r}) + (\omega_{TO}^{\alpha})^{2}u_{\alpha}^{2}(\vec{r}) - \beta_{12}^{\alpha}E_{\alpha}(\vec{r})u_{\alpha}(\vec{r})], \tag{34}$$

where $\Pi_{\alpha}(\vec{r})$ is the α component of the momentum density canonically conjugated to the phonon field component $u_{\alpha}(\vec{r})$. $\vec{E}(\vec{r})$ is the intensity of the macroscopic electric field created by both, surface and volume, polarization charges.

As an important step in the procedure developed to obtain the final form of H_{ph} that includes the contributions of all types of the phonon modes, the orthogonality relation (32) for the eigenvectors of the phonon field will be used.

Now, in the following, we shall consider $\vec{\Pi}(\vec{r})$ and $\vec{u}(\vec{r})$ as field operators written in the Schrödinger picture. Thus, the operator $\vec{u}(\vec{r})$ can be written in terms of the phonon normal modes (m,q,l,μ):

$$\vec{u}(\vec{r}) = \sum_{mql\mu} \lambda_{mql}^{(\mu)}[\vec{u}_{mql}^{(\mu)}(\vec{r})a_{mql}^{(\mu)} + \text{H.c.}], \tag{35}$$

where, without loosing the generality of the problem, the quantities $\lambda_{mql}^{(\mu)}$ are considered to be real, depending on $|m|$ and $|q|$; $a_{mql}^{(\mu)}$ and $a_{mql}^{(\mu)^{+}}$ are the annihilation and creation operators for the phonon mode (m,q,l,μ). The operators $a_{mql}^{(\mu)}$ and $a_{mql}^{(\mu)^{+}}$ verify typical Bose commutation relations:

$$[a_{mql}^{(\mu)}, a_{m'q'l'}^{(\mu')}] = 0, \quad [a_{mql}^{(\mu)^{\dagger}}, a_{m'q'l'}^{(\mu')^{\dagger}}] = 0,$$

$$[a_{mql}^{(\mu)}, a_{m'q'l'}^{(\mu')^{\dagger}}] = \delta_{mm'}\delta_{ll'}\delta_{qq'}\delta_{\mu\mu'}. \tag{36}$$

For the purpose of putting the phonon Hamiltonian into the form

$$H_{ph} = \sum_{mql\mu} \hbar\omega_{mql}^{(\mu)} \left[a_{mql}^{(\mu)\dagger} a_{mql}^{(\mu)} + \frac{1}{2} \right], \tag{37}$$

we make use of the classical equation of motion[37]

$$\vec{\Pi} = \dot{\vec{u}} \tag{38}$$

to derive the following development in the Schrödinger picture for the operator $\vec{\Pi}$:

$$\vec{\Pi}(\vec{r}) = -i \sum_{mql\mu} \lambda_{mql}^{(\mu)} \omega_{mql}^{(\mu)} [\vec{u}_{mql}^{(\mu)}(\vec{r}) a_{mql}^{(\mu)} - \text{H.c.}]. \tag{39}$$

To be consistent with the notations used to differentiate between various types of the phonon normal modes, we have to assign $l=1$ for the surface modes in the following notations: $\omega_{mq1}^{(0)} = \omega_{mq}^{(0)}$ and $\vec{u}_{mq1}^{(0)}(\vec{r}) = \vec{u}_{mq}^{(0)}(\vec{r})$.

By using expression (35) of the operator $\vec{u}(\vec{r})$, the α component of the electric field operator in Eq. (1) can be put in the form

$$E_\alpha(\vec{r}) = \sum_{mql\mu} \lambda_{mql}^{(\mu)} \frac{(\omega_{TO}^{\alpha})^2 - [\omega_{mql}^{(\mu)}]^2}{\beta_{12}^{\alpha}} \{[\vec{u}_{mql}^{(\mu)}(\vec{r})]_\alpha a_{mql}^{(\mu)} + \text{H.c.}\}, \tag{40}$$

with $\alpha = \parallel$ and $\perp$.

Now, the phonon Hamiltonian density given by Eq. (34) is fully solved with the use of expressions (35), (39), and (40), and the free phonon Hamiltonian

$$H_{ph} = \int_V dV h_{ph}(\vec{r}) \tag{41}$$

can be converted into form (37) by making the simple notation

$$\lambda_{mql}^{(\mu)} = \left(\frac{\hbar}{2\omega_{mql}^{(\mu)}} \right)^{1/2}. \tag{42}$$

Next, we derive the interaction Hamiltonian between the conduction electron and the optical phonon field (Fröhlich interaction). This interaction is due to both types of polarization charges which contribute to the electrostatic potential, the volume charges and the surface charges. Simply, it may be written as

$$H_{e\text{-}ph} = e\Phi(\vec{r}), \quad e < 0, \tag{43}$$

e being the electron charge and $\Phi(\vec{r})$ the electrostatic potential including the above specified contributions.

The different phonon mode contributions to this Hamiltonian will be obtained by developing the electrostatic potential in terms of eigenvectors of the phonon field. By taking into account solution (17) for the electrostatic potential, the development (35) of the phonon vector field, and expression (42) of the constant $\lambda_{mql}^{(\mu)}$, the electron-phonon interaction Hamiltonian is obtained in the form

$$H_{e\text{-}ph} = -\sum_{mql\mu} \Gamma_{ml}^{(\mu)}(q) [W_{mq}(z,\varphi) g_{qlm}^{(\mu)}(|q|\rho) a_{mql}^{(\mu)} + \text{H.c.}]. \tag{44}$$

The coupling functions $\Gamma_{ml}^{(\mu)}(q)$ and the functions $g_{qlm}^{(\mu)}(|q|\rho)$ in Eq. (44) are specified by the type of the involved optical phonon modes as follows:

(a) for surface modes ($\mu=0, l=1$)

$$\Gamma_{m1}^{(0)}(q) = \frac{\left(\frac{\hbar e^2}{|q|R\varepsilon_0} \right)^{1/2}}{\left| \left[I_{|m|}\left(\frac{|q|R}{\sqrt{s}} \right) I'_{|m|}\left(\frac{|q|R}{\sqrt{s}} \right) \frac{\partial f_{mq}^{(0)}(\omega)}{\partial\omega} \right]_{\omega=\omega_{mq}^{(0)}} \right|^{1/2}}, \tag{45}$$

$$g_{qml}^{(0)}(|q|\rho) = I_{|m|}\left(\frac{|q|\rho}{\sqrt{s(\omega_{mq}^{(0)})}} \right); \tag{46}$$

(b) for confined modes ($\mu=1,2$)

$$\Gamma_{ml}^{(\mu)}(q) = \frac{\left(\frac{\hbar e^2}{|q|R\varepsilon_0} \right)^{1/2}}{\left| \left[J_{|m|}\left(\frac{|q|R}{\sqrt{|s|}} \right) J'_{|m|}\left(\frac{|q|R}{\sqrt{|s|}} \right) \frac{\partial f_{mql}^{(\mu)}(\omega)}{\partial\omega} \right]_{\omega=\omega_{mql}^{(\mu)}} \right|^{1/2}}, \tag{47}$$

$$g_{qml}^{(\mu)}(|q|\rho) = J_{|m|}\left(\frac{|q|\rho}{\sqrt{|s(\omega_{mql}^{(\mu)})|}} \right). \tag{48}$$

The behavior of the coupling function $\Gamma_{ml}^{(\mu)}(q)$ for all types of the optical phonon modes is shown in Figs. 2(a) and 2(b) for ZnO and GaN, respectively. Once again, only the coupling functions for the phonon modes with $|m| \leqslant 2, l=1$ and 2, and $\mu=0$, 1, and 2, are plotted. As can be seen, unlike the case of an isotropic wire when the transverse phonon modes do not interact with a conduction electron, for uniaxial anisotropic wires, the quasitransverse-phonon modes interact with electrons. The values of the coupling function $\Gamma_{lm}^{(2)}(|q|R)$ for quasilongitudinal modes are over an order of magnitude higher than the corresponding values of coupling function $\Gamma_{lm}^{(1)}(|q|R)$ for quasitransverse modes. At relatively small values of $|q|R$, the strength of the interaction between electrons and the surface phonon modes is comparable with that involving the quasilongitudinal-phonon modes.

The continuity of the coupling function $\Gamma_{01}^{(0)}(|q|R)$ when the character of the phonon modes changes from surface into quasitransverse is observed.

V. POLARON IN ANISOTROPIC QUANTUM WIRE

The previously obtained results are used in this section to obtain the self-energy and the effective mass of an optical polaron in our anisotropic QWR. The Fröhlich Hamiltonian we have derived for a uniaxial crystal is an extension, to this anisotropic case, of the Hamiltonian previously introduced in

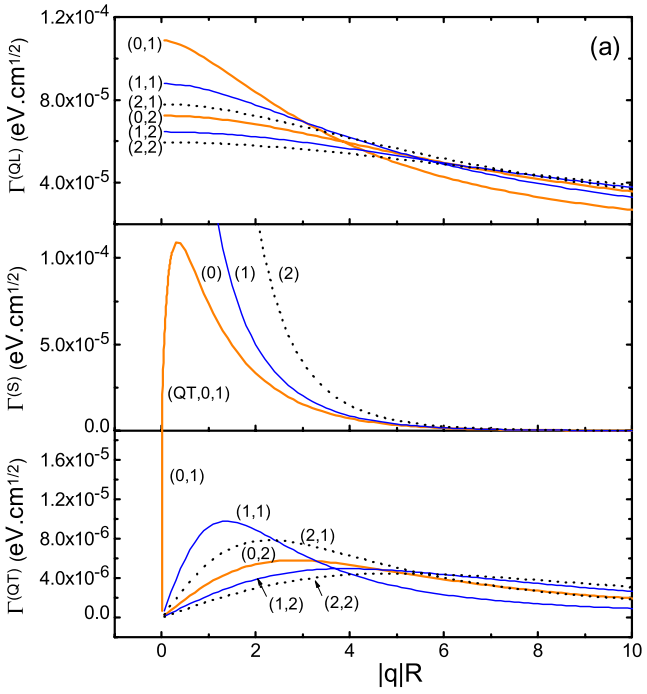

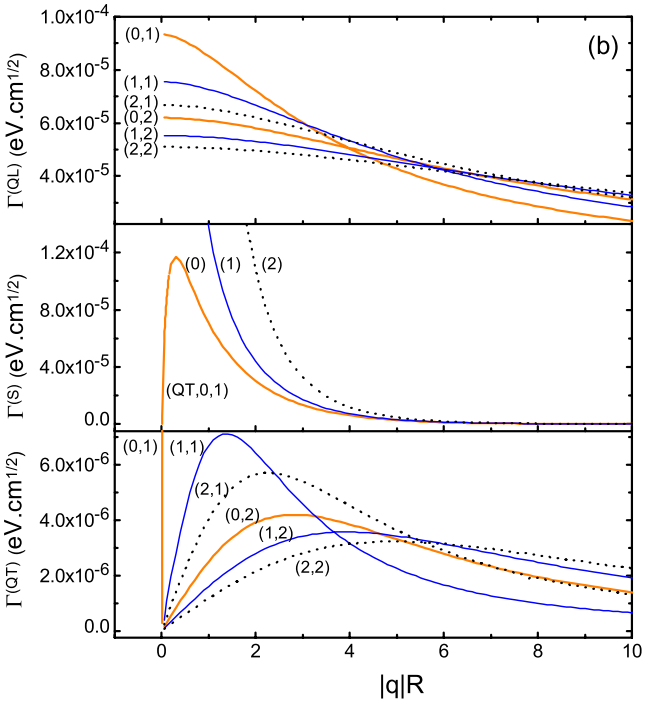

FIG. 2. (Color online) Coupling functions $\Gamma_{ml}^{(\mu)}(q)$ for (a) ZnO and (b) GaN QWRs, plotted with orange (gray) solid line for $m=0$, blue (black) solid line for $|m|=1$, and black dotted line for $|m|=2$. The quantum numbers (m,l) of the phonon modes are indicated on the plot.

Ref. 38 for a QWR made of isotropic materials. The polaron renormalization effects including the contributions of all types of phonons will be found in the frame of the Rayleigh-Schrödinger perturbation theory.

The polaron Hamiltonian is

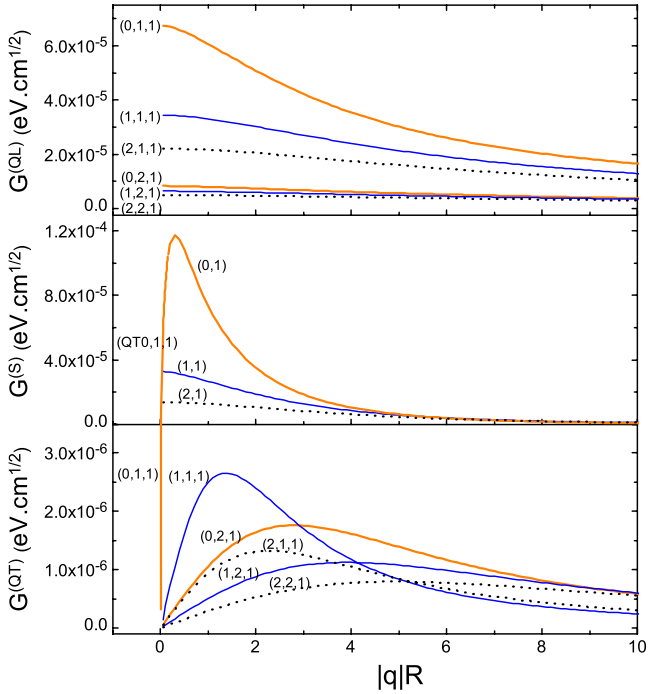

FIG. 3. (Color online) The matrix elements $G_{ml,s}^{(\mu)}(q)$ of a few phonon branches for GaN wire, plotted with orange (gray) solid line for $m=0$, blue (black) solid line for $|m|=1$, and black dotted line for $|m|=2$. The quantum numbers (m,l) of the phonon modes are indicated on the plot.

$$H = H_e + H_{ph} + H_{e\text{-}ph}, \tag{49}$$

where for the Hamiltonian of the electron we shall consider the form

$$H_e = \frac{\vec{p}_\parallel^{\,2}}{2m_\parallel} + \frac{\vec{p}_\perp^{\,2}}{2m_\perp} + V(\rho). \tag{50}$$

In the above expression, $p_\parallel$ and $p_\perp$ are the components of the electron momentum along a direction that is either parallel ($\parallel$) or orthogonal ($\perp$) to the optical axis, $m_\parallel$ and $m_\perp$ being the corresponding components of the diagonal mass tensor for the conduction electron. $V(\rho)$ is the electron confinement potential defined for a cylindrical quantum well wire by $V(\rho)=0$ for $\rho \leqslant R$, and $V(\rho)=\infty$ otherwise.

The electron state $|k,M,s\rangle$ with the wave function[39]

$$\Psi_{kMs}(\vec{r}) = \left(\frac{2}{R^2}\right)^{1/2} \frac{J_{|M|}\left(\frac{\gamma_{|M|s}}{R}\rho\right)}{|J_{|M|+1}(\gamma_{|M|s})|} W_{Mk}(z,\varphi) \tag{51}$$

and the energy

$$E_{Ms}(k) = \frac{\hbar^2 k^2}{2m_\parallel} + \frac{\hbar^2}{2m_\perp}\left(\frac{\gamma_{|M|s}}{R}\right)^2 \tag{52}$$

depend on the following quantum numbers: k the wave vector component along the optical axis, having the values determined from the periodic boundary conditions; M the angular quantum number $(M=0,\pm1,\pm2,\ldots)$; and s the radial

quantum number which corresponds to the sth zero of the Bessel function of order $|M|$ according to the relation

$$J_{|M|}(\gamma_{|M|s}) = 0. \tag{53}$$

The energy values of the electric subbands ($|M|s$) verify, for the same value of k, the following inequalities:[39]

$$E_{01}(k) < E_{11}(k) < E_{21}(k) < E_{02}(k) < E_{31}(k) < E_{12}(k) < E_{41}(k) < E_{03}(k). \tag{54}$$

We assume the system to be at zero temperature and the electron in the unperturbed state $|k,0,1\rangle$ of the first electric subband. Thus, the initial state of the total system is $|\Psi_i\rangle = |k,0,1\rangle \otimes |0_{ph}\rangle$, where the vacuum state of the phonon system was denoted by $|0_{ph}\rangle$. With these assumptions, according to the phonon-emission process, the intermediate state is

$$|\Psi_\lambda\rangle = |k-q,-m,s\rangle \otimes |1_{ph}(q,m,l,\mu)\rangle. \tag{55}$$

The energy of the polaron can then be obtained in the second order of the Rayleigh-Schrödinger perturbation series as

$$E_{pol}(k) = E_{01}(k) + \sum_\lambda \frac{|\langle\Psi_\lambda|H_{e\text{-}ph}|\Psi_i\rangle|^2}{E_i - E_\lambda}. \tag{56}$$

The matrix element appearing in Eq. (56) has the form

$$\langle\Psi_\lambda|H_{e\text{-}ph}|\Psi_i\rangle = -\frac{G^{(\mu)}_{ml;s}(q)}{\sqrt{2\pi L}}, \tag{57}$$

where

$$G^{(\mu)}_{ml;s}(q) = 2\Gamma^{(\mu)}_{ml}(q)\int_0^1 zdz \frac{J_{|m|}(\gamma_{|m|s}z)g^{(\mu)}_{qml}(z|q|R)J_0(\gamma_{01}z)}{|J_{|m|+1}(\gamma_{|m|s})J_1(\gamma_{01})|}. \tag{58}$$

In Fig. 3, the matrix element $G^{(\mu)}_{ml;s}(q)$ is shown for GaN as a function of $|q|R$; only the values $|m| \leqslant 2$; $l=1$ and $2, \mu=0$, 1, and 2; and $s=1$ have been considered here. One can see that the behavior of this matrix element is similar to that of $\Gamma^{(\mu)}_{ml}(q)$ [which is shown in Fig. 2(b)]. The surface mode contributions for $|m| \leqslant 2$ are comparable with those of the quasilongitudinal modes for $|m| \leqslant 2$ and $l=1$. However, the contributions of the quasitransverse modes are 1 order of magnitude lower. By taking into account relations (52), (56), and (57), the expression of the polaron energy is

$$E_{pol}(k) = E_{01}(k) - \frac{1}{2\pi L}\sum_{mqls\mu} \frac{|G^{(\mu)}_{ml;s}(q)|^2}{\hbar\omega^{(\mu)}_{ml}(q) + \frac{\hbar^2}{2m_\parallel}(q^2-2kq) + \frac{\hbar^2}{2m_\perp}\left[\left(\frac{\gamma_{|m|s}}{R}\right)^2 - \left(\frac{\gamma_{01}}{R}\right)^2\right]}. \tag{59}$$

By using relation (59), the expressions of the quantities of interest, such as the self-energy of the polaron (E_s) and the effective mass of the polaron (M_p), are obtained:

$$E_s = E_{pol}(0) - E_{01}(0), \tag{60}$$

$$M_p = \frac{m_\parallel}{1 - 4\left(\frac{2m_\parallel}{\hbar^2}\right)^2 \frac{1}{2\pi L}\sum_{m,q,l,s,\mu} \frac{q^2|G^{(\mu)}_{m,l;s}(q)|^2}{\left\{q^2 + \frac{m_\parallel}{m_\perp}\left[\left(\frac{\gamma_{|m|s}}{R}\right)^2 - \left(\frac{\gamma_{01}}{R}\right)^2\right] + \frac{2m_\parallel}{\hbar^2}\omega^{(p)}_m(q)\right\}^3}}. \tag{61}$$

In the following, the values of the polaron self-energy and polaron effective mass as a function of the wire radius R are calculated for the phonon branches $|m| \leqslant 3$; $l=1$, 2, and 3; and $\mu=0$, 1, and 2; and the corresponding electronic states with $|M| \leqslant 3$ and $s=1$, 2, and 3, with the values[40] $m_\parallel = 0.20m_0$ and $m_\perp = 0.20m_0$ for the components of the effective mass tensor of the bare electron.

Figure 4 shows the self-energy of the polaron, E_s, including the contributions of the states mentioned above as a function of the radius of the wire. For comparison purposes, two curves are shown, the polaron energy values calculated by including the contributions of the states $|m| \leqslant 2$; $l,s \leqslant 2$; and $\mu=0$, 1, and 2 (open squares), and of the states $|m| \leqslant 3$; $l,s \leqslant 3$; and $\mu=0$, 1, and 2 (filled squares), respectively. As one can see, there are no significant differences for $R<4$ nm; in fact, for a wire having a radius $R=4$ nm, the relative difference is about 4.4%. We can conclude that for smaller radii, the performed numerical evaluations of the polaron self-energy lead to acceptable results. Concerning the radius dependence of the polaron effective mass, we have observed that there are no differences between the curves calculated with the inclusion of the above mentioned terms. That behavior is determined by the fact that the summation terms containing energy differences in the denominator of Eq. (61) are cubic. The value of the self-energy of a 3D polaron ($E_s = -42.03$ meV) is also specified on the plot. This is calcu-

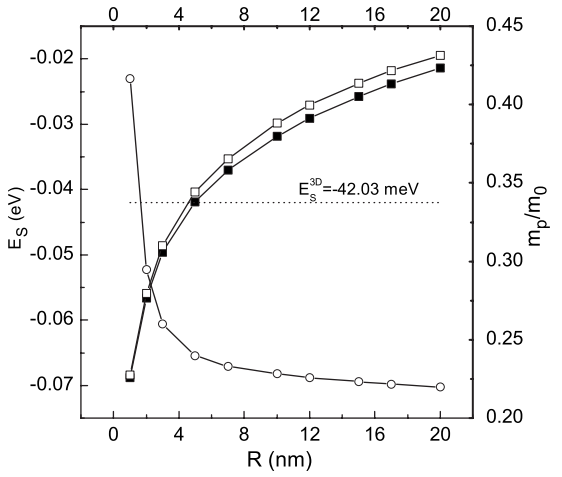

FIG. 4. The self-energy (open squares for $|m| \leqslant 2$; $l,s \leqslant 2$; $\mu = 0$, 1, and 2; and filled squares for $|m| \leqslant 3$; $l,s \leqslant 3$; and $\mu = 0$, 1, and 2) and polaron mass (open circles) as function of wire radius in a GaN QWR.

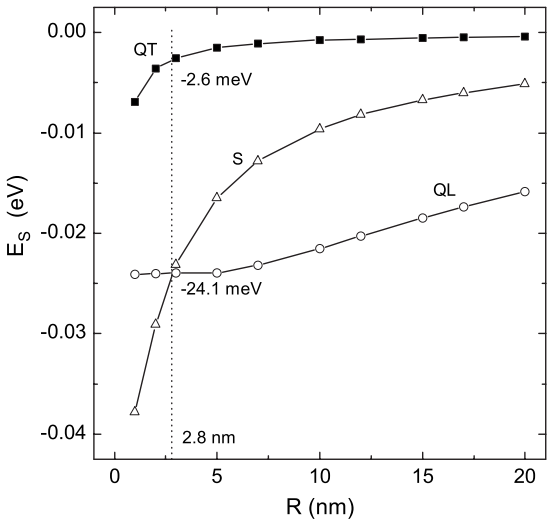

FIG. 5. The contribution to the polaron self-energy for different types (QL, quasilongitudinal; QT, quasitransverse; and S, surface) of phonon modes.

lated by considering the anisotropic forms of the so-called dimensionless Fröhlich polaron constants.[37] For this material, there are two such quantities, denoted by α_1 and α_2 for quasitransverse- and quasilongitudinal-phonon modes, respectively. These quantities depend on the angle θ formed by the 3D phonon wave vector with the optical axis; their angular average values are $\langle \alpha_1(\theta) \rangle = 0.002$ and $\langle \alpha_2(\theta) \rangle = 0.456$. We have to stress that, in some circumstances, like magnetopolaron resonance in 2D anisotropic uniaxial systems,[41] such small coupling between the conduction electron and the quasitransverse optical phonons can lead to important effects.

Because in the process of evaluating the self-energy we have used only a small part of the set of intermediate states, the 3D value is not obtained for $R \to \infty$; this fact limiting our results to the case of wires with very small radius ($R < 4$ nm). Of course, the results could be improved by enlarging the number of the intermediate states taken into consideration. In the particular case of a parabolic confinement potential, we have succeeded to sum[41] the contributions of all the intermediate states for a 2D system and the correct 3D limit has been obtained.

The polaron problem in asymmetric quantum well structures was analyzed in Ref. 42 by using second-order perturbation theory and the modified Lee-Low-Pines variational method. By taking into account the contributions of the full energy spectrum, the authors have pointed the importance of including the continuum part of the spectrum for obtaining correct values of the polaron self-energy in the whole range of well widths. The same perturbative approach was used to obtain the polaron self-energy and the polaron effective mass in a free-standing cylindrical quantum wire made of an isotropic material.[43] It seems that the author succeeded to evaluate correctly the contributions of all intermediate states to the polaron self-energy and effective mass. As the radius of the wire increases, both quantities of interest reach the corresponding 3D values. At small values of the wire radius, our results regarding the dependence of the self-energy on the wire radius are similar to those reported in Ref. 43.

The same polaron problem in the case of a cylindrical wire embedded in a polar medium (the two materials being isotropic) was addressed in Ref. 44. Due to both the finiteness of the confining potential and the presence of the barrier material, the behavior of the contributions of the interface phonons to the polaron self-energy and effective mass is different from that obtained in the case of a free-standing quantum wire. Such an approach could be useful for a future study of the polaron problem in a uniaxial anisotropic quantum wire embedded in an anisotropic medium.

In Fig. 5, the contributions of different phonon modes with the same character to the polaron self-energy are calculated as function of wire radius (up triangles for surface modes, circles for quasilongitudinal modes, and squares for quasitransverse modes). The considered states are those corresponding to the quantum numbers $|m|$, $|M| \leqslant 2$ and $l,s \leqslant 2$. For QWRs with radius smaller than 2.8 nm, the surface mode contribution to the polaron self-energy becomes the most important one. Also, for this confined system ($R = 2.8$ nm), the quasitransverse mode contribution to the polaron self-energy (−2.6 meV) is 1 order of magnitude greater (in absolute value) than the same contribution (−0.18 meV) for a 3D crystal, those differences being larger for smaller wire radius.

The approach developed in this paper to study the dispersion laws of the optical phonon modes and their interaction with a conduction electron in anisotropic uniaxial QWRs can be easily extended to the case of q-1D heterostructures made of anisotropic uniaxial materials.

VI. SUMMARY

In the context of the DC model, the dispersion laws of full optical phonon spectrum for a uniaxial anisotropic QWR made of wurtzite-type material and their interaction Hamil-

tonian with a conduction electron are obtained. Unlike the situation found in isotropic QWRs, the degeneracy of the confined (longitudinal and transverse) modes is raised for an anisotropic uniaxial QWR. Thus, for the particular case of wurtzite-type materials, the confined modes show dispersion and have their frequencies distributed in two distinct intervals, one of the longitudinal-phonon modes $[\omega \in (\omega_{LO}^{\parallel}, \omega_{LO}^{\perp})]$ and one of the quasitransverse-phonon modes $[\omega \in (\omega_{TO}^{\parallel}, \omega_{TO}^{\perp})]$. For one specific quasitransverse-phonon branch, it has been found that its character changes into that of a surface branch starting at a threshold value of the wave vector. Also, the coupling function describing the electron-phonon interaction, for all types of optical phonons (quasilongitudinal, quasitransverse, and surface), is obtained in an analytical closed form, which is, mainly, determined by the dispersion law of the phonon modes involved. Unlike the case of isotropic systems, in anisotropic QWRs, the quasitransverse-phonon modes interact with conduction electrons in the same way as in 3D uniaxial crystals and other low-dimensional systems. Similar to the continuity property of the dispersion law when a phonon branch changes its character (e.g., from quasitransverse to surface type), the continuity of the corresponding coupling function has been demonstrated here. As practical applications, numerical calculations for ZnO and GaN QWRs have been performed. Though small compared with the strength of the interaction between an electron and surface and quasilongitudinal phonons, the electron-quasitransverse-phonon interaction can yield, in some circumstances, important effects. We have demonstrated the orthogonality relation between the eigenvectors of the phonon field and used this to obtain the expression of the complete Fröhlich Hamiltonian for our system. Finally, we have discussed, in the second order of perturbation theory, the polaron problem in GaN QWR with infinitely deep potential. The dependences of the self-energy and effective mass of the polaron on the radius of the wire have been obtained. The contribution of the surface modes to the polaron self-energy becomes significant for thin QWR ($R < 2.8$ nm). A ten times larger contribution (and this could be even larger for smaller radii) of the quasitransverse modes to the polaron energy is found in a GaN QWR with $R = 2.8$ nm than in a similar 3D crystal. All the obtained results could be extended to the case of an anisotropic QWR embedded into a nonpolar isotropic (anisotropic) material having a dielectric constant $\varepsilon^H(\varepsilon_{\parallel}^H, \varepsilon_{\perp}^H)$ by replacing $\varepsilon_{\parallel}(\infty)$ and $\varepsilon_{\perp}(\infty)$ everywhere by $\frac{\varepsilon_{\parallel}(\infty)}{\varepsilon^H}$, $\frac{\varepsilon_{\perp}(\infty)}{\varepsilon^H}$, and $\left(\frac{\varepsilon_{\parallel}(\infty)}{\varepsilon_{\parallel}^H}, \frac{\varepsilon_{\perp}(\infty)}{\varepsilon_{\perp}^H}\right)$.

APPENDIX A: ORTHOGONALITY RELATION BETWEEN TWO VECTORS OF THE PHONON FIELD HAVING DIFFERENT FREQUENCIES

Equation (12) can be written in the general form

$$\sum_{i,j} \frac{\partial}{\partial x_i}\left[\varepsilon_{ij}(\omega)\frac{\partial \Phi(\vec{r},\omega)}{\partial x_j}\right] = 0. \tag{A1}$$

By multiplying the left side of Eq. (12) with $\Phi^*(\vec{r},\omega')$ and integrating over the system volume, we obtain

$$\int_V dV \Phi^*(\vec{r},\omega') \sum_{i,j} \frac{\partial}{\partial x_i}\left[\varepsilon_{ij}(\omega)\frac{\partial \Phi(\vec{r},\omega)}{\partial x_j}\right] = 0. \tag{A2}$$

Expression (A2) can be further developed with the help of the Gauss theorem, resulting in

$$\int_V dV \sum_{i,j} \frac{\partial \Phi^*(\vec{r},\omega')}{\partial x_i}\varepsilon_{ij}(\omega)\frac{\partial \Phi(\vec{r},\omega)}{\partial x_j} = \oint_\Sigma d\sigma \Phi^*(\vec{r},\omega') \sum_{i,j}\left[n_i \varepsilon_{ij}(\omega)\frac{\partial \Phi(\vec{r},\omega)}{\partial x_j}\right], \tag{A3}$$

n_i being the i component of the unit vector parallel to the outward normal from the surface (Σ) of the system. Now, by taking the complex conjugate of Eq. (1) written for ω' and considering the fact that matrix ε is a real and symmetrical matrix, the following simple expression is obtained:

$$\sum_{i,j} \frac{\partial}{\partial x_j}\left[\frac{\partial \Phi^*(\vec{r},\omega')}{\partial x_i}\varepsilon_{ij}(\omega')\right] = 0. \tag{A4}$$

By multiplying the left side of relation (A4) by $\Phi(\vec{r},\omega)$ and applying the Gauss theorem, we get the relation

$$\int_V dV \sum_{i,j} \frac{\partial \Phi(\vec{r},\omega)}{\partial x_j}\varepsilon_{ij}(\omega')\frac{\partial \Phi^*(\vec{r},\omega')}{\partial x_i} = \oint_\Sigma d\sigma \Phi(\vec{r},\omega) \sum_{i,j}\left[n_j \varepsilon_{ij}(\omega')\frac{\partial \Phi^*(\vec{r},\omega')}{\partial x_i}\right]. \tag{A5}$$

By taking into account relations (15) and (16) and the symmetry of the matrix ε, it is easy to see that the two surface integrals appearing in Eqs. (A3) and (A5) are equal and have the value

$$J_\Sigma = \sum_{mq} |B_{mq}|^2 |q| K_m(R|q|) |K_m'(R|q|). \tag{A6}$$

Thus, the result of subtracting Eq. (A3) from Eq. (A5) leads to

$$\int_V dV \sum \frac{\partial \Phi^*(\vec{r},\omega')}{\partial x_i}[\varepsilon_{ij}(\omega) - \varepsilon_{ij}(\omega')]\frac{\partial \Phi(\vec{r},\omega)}{\partial x_j} = 0. \tag{A7}$$

Now, by taking into account relationship (14), the left hand term of the above expression can be written in terms of the components $\vec{u}_{\parallel}$ and $\vec{u}_{\perp}$ of the phonon vector field:

$$\sum_{\alpha=\parallel,\perp} [\varepsilon_\alpha(\omega) - \varepsilon_\alpha(\omega')] g_\alpha(\omega) g_\alpha(\omega') \int_V dV \vec{u}_\alpha^*(\vec{r},\omega') \vec{u}_\alpha(\vec{r},\omega) = 0. \tag{A8}$$

Based on Eqs. (3) and (6), relation (A8) can be put into the remarkable form

$$[\omega^2 - (\omega')^2] \int_V dV \vec{u}^*(\vec{r},\omega') \vec{u}(\vec{r},\omega) = 0. \tag{A9}$$

This means that any two vectors of the phonon field having different frequencies are orthogonal.

APPENDIX B: EXPRESSION OF THE NORMALIZATION CONSTANT $C_{mq}^{(0)}$

By taking into account expressions (24) and (25) of the components of the normal mode $(m,q,0)$, one obtains

$$\frac{1}{|C_{mq}^{(0)}|^2} = \int_0^R \rho d\rho \left[\frac{q^2}{g_\parallel^2(\omega_{mq}^{(0)})} I_{|m|}^2\left(\frac{|q|\rho}{\sqrt{s}}\right) + \frac{1}{g_\perp^2(\omega_{mq}^{(0)})}\left\{ \frac{m^2}{\rho^2} I_{|m|}^2\left(\frac{|q|\rho}{\sqrt{s}}\right) + \frac{q^2}{s}\left[I'_{|m|}\left(\frac{|q|\rho}{\sqrt{s}}\right)\right]^2\right\}\right]. \tag{B1}$$

To simplify the presentation, in the following, we shall write ω instead of $\omega_{mq}^{(0)}$ and we shall denote by λ the ratio $\frac{|q|}{\sqrt{s}}$. We shall calculate separately the last integral of expression (B1). Integrating by parts, one obtains

$$\int_0^R \rho d\rho [I'_{|m|}(\lambda\rho)]^2 = \frac{R}{\lambda} I'_{|m|}(\lambda R) I_{|m|}(\lambda R) - \int_0^R \rho d\rho I_{|m|}(\lambda\rho) \times \left[I''_{|m|}(\lambda\rho) + \frac{1}{\lambda\rho} I'_{|m|}(\lambda\rho)\right]. \tag{B2}$$

Based on the Bessel equation written for $I_{|m|}(\lambda\rho)$:

$$I''_{|m|}(\lambda\rho) + \frac{1}{\lambda\rho} I'_{|m|}(\lambda\rho) - \left(1 + \frac{m^2}{\lambda^2\rho^2}\right) I_{|m|}(\lambda\rho) = 0, \tag{B3}$$

the integral (B2) becomes

$$\int_0^R \rho d\rho [I'_{|m|}(\lambda\rho)]^2 = \frac{R}{\lambda} I'_{|m|}(\lambda R) I_{|m|}(\lambda R) - \int_0^R \rho d\rho \left(1 + \frac{m^2}{\lambda^2\rho^2}\right) I_{|m|}^2(\lambda\rho). \tag{B4}$$

By taking into account relation (B4), expression (B1) simplifies to

$$\frac{1}{|C_{mq}^{(0)}|^2} = \frac{R\lambda}{g_\perp^2(\omega)} I'_{|m|}(\lambda R) I_{|m|}(\lambda R) + q^2\left[\frac{1}{g_\parallel^2(\omega)} - \frac{1}{s g_\perp^2(\omega)}\right] \int_0^R \rho d\rho I_{|m|}^2(\lambda\rho). \tag{B5}$$

The integral appearing in Eq. (B5), known as one of the Lommel integrals, can be performed,[33] obtaining

$$\int_0^R \rho d\rho I_{|m|}^2(\lambda\rho) = -\frac{R^2}{2}\{[I'_{|m|}(\lambda R)]^2 - I_{|m|}(\lambda R) I''_{|m|}(\lambda R)\} + \frac{R}{2\lambda} I_{|m|}(\lambda R) I'_{|m|}(\lambda R). \tag{B6}$$

In these circumstances, expression (B5) becomes

$$\frac{1}{|C_{mq}^{(0)}|^2} = \frac{|q|R}{2}\left[\frac{1}{\sqrt{s} g_\perp^2(\omega)} + \frac{\sqrt{s}}{g_\parallel^2(\omega)}\right] I'_{|m|}(\lambda R) I_{|m|}(\lambda R) - \frac{q^2R^2}{2}\left[\frac{1}{g_\parallel^2(\omega)} - \frac{1}{g_\perp^2(\omega)}\right]\{[I'_{|m|}(\lambda R)]^2 - I_{|m|}(\lambda R) I''_{|m|}(\lambda R)\}. \tag{B7}$$

Now, by replacing the functions $g_\parallel^2(\omega)$ and $g_\perp^2(\omega)$ in terms of the derivatives $\frac{\partial\varepsilon_\parallel(\omega)}{\partial\omega}$ and $\frac{\partial\varepsilon_\perp(\omega)}{\partial\omega}$ by considering the relations

$$\frac{1}{g_{\parallel,\perp}^2(\omega)} = \frac{\varepsilon_0}{2\omega}\frac{\partial\varepsilon_{\parallel,\perp}(\omega)}{\partial\omega}, \tag{B8}$$

expression (B7) can be put in the form

$$\frac{1}{|C_{mq}^{(0)}|^2} = \frac{q^2R^2}{4\omega}\frac{\varepsilon_0}{\varepsilon_\perp}\left(\varepsilon_\parallel\frac{\partial\varepsilon_\perp}{\partial\omega} - \varepsilon_\perp\frac{\partial\varepsilon_\parallel}{\partial\omega}\right)\{[I'_{|m|}(\lambda R)]^2 - I_{|m|}(\lambda R) I''_{|m|}(\lambda R)\} - \frac{|q|R}{4\omega}\frac{\varepsilon_0}{\sqrt{\varepsilon_\perp\varepsilon_\parallel}} \times\left(\varepsilon_\parallel\frac{\partial\varepsilon_\perp}{\partial\omega} + \varepsilon_\perp\frac{\partial\varepsilon_\parallel}{\partial\omega}\right) I'_{|m|}(\lambda R) I_{|m|}(\lambda R). \tag{B9}$$

Now, a straightforward calculation, which involves the dispersion law Eq. (22), allows us to express the right member of relation (B9) in terms of the derivative of the function $f_{mq}^{(0)}(\omega)$, which was defined in Eq. (23).

Returning to the initial variables $\omega_{mq}^{(0)}$ and $\frac{|q|}{\sqrt{s}}$, expression (B9) becomes

$$\frac{1}{|C_{mq}^{(0)}|^2} = \frac{\varepsilon_0|q|R}{2\omega_{mq}^{(0)}}\left[I_{|m|}\left(\frac{|q|R}{\sqrt{s}}\right) I'_{|m|}\left(\frac{|q|R}{\sqrt{s}}\right)\frac{\partial f_{mq}^{(0)}(\omega)}{\partial\omega}\right]_{\omega=\omega_{mq}^{(0)}}. \tag{B10}$$

By dropping out a possible phase factor, form (26) for the normalization constant $C_{mq}^{(0)}$ is obtained.

*dane@solid.fizica.unibuc.ro
†lucian@solid.fizica.unibuc.ro

[1] R. Loudon, Adv. Phys. **13**, 423 (1964).
[2] K. Huang and B. F. Zhu, Phys. Rev. B **38**, 13377 (1988).
[3] H. Rucker, E. Molinari, and P. Lugli, Phys. Rev. B **44**, 3463 (1991); **45**, 6747 (1992).
[4] P. Bordone and P. Lugli, Phys. Rev. B **49**, 8178 (1994).
[5] A. K. Sood, J. Menendez, M. Cardona, and K. Ploog, Phys. Rev. Lett. **54**, 2115 (1985).
[6] R. Hessmer, A. Huber, T. Egeler, M. Haines, G. Trankle, G. Weimann, and G. Abstreiter, Phys. Rev. B **46**, 4071 (1992).
[7] S. Nakamura and G. Fasol, *The Blue Laser Diode* (Springer-Verlag, Berlin, 1997).
[8] B. Gil, *Group III Nitride Semiconductor Compounds* (Clarendon,

Oxford, 1998).
[9] S. Nakamura and S. F. Chichibu, *Introduction to Nitride Semiconductor Blue Lasers and Light Emitting Diodes* (Taylor & Francis, London, 2000).
[10] E. R. Racec and D. E. N. Brancus, J. Phys.: Condens. Matter **10**, 3845 (1998).
[11] B. C. Lee, K. W. Kim, M. A. Stroscio, and M. Dutta, Phys. Rev. B **58**, 4860 (1998).
[12] S. M. Komirenko, K. W. Kim, M. A. Stroscio, and M. Dutta, Phys. Rev. B **59**, 5013 (1999).
[13] J. Gleize, M. A. Renucci, J. Frandon, and F. Demangeot, Phys. Rev. B **60**, 15985 (1999).
[14] J.-J. Shi, Phys. Rev. B **68**, 165335 (2003).
[15] J.-J. Shi, X.-L. Chu, and E. M. Goldys, Phys. Rev. B **70**, 115318 (2004).
[16] D. A. Romanov, V. V. Mitin, and M. A. Stroscio, Physica B **316-317**, 359 (2002).
[17] D. A. Romanov, V. V. Mitin, and M. A. Stroscio, Phys. Rev. B **66**, 115321 (2002).
[18] D. A. Romanov, V. V. Mitin, and M. A. Stroscio, Physica E (Amsterdam) **12**, 491 (2002).
[19] J. Gleize, J. Frandon, F. Demangeot, M. A. Renucci, C. Adelmann, B. Dandin, G. Feuillet, B. Damilano, N. Grandjean, and J. Massies, Appl. Phys. Lett. **77**, 2174 (2000).
[20] M. H. Huang, S. Mao, H. Fieck, H. Yan, Y. Wu, H. Kind, E. Weber, R. Richard, and P. Yang, Science **292**, 5523 (2001).
[21] J. C. Johnson, H. J. Choi, K. P. Knutsen, R. D. Schaller, P. D. Yang, and R. J. Saykally, Nat. Mater. **1**, 106 (2002).
[22] H. J. Choi, J. C. Johnson, R. He, S. K. Lee, F. Kim, P. Panzanskie, J. Goldberger, R. J. Saykally, and P. Yang, J. Phys. Chem. B **107**, 8271 (2003).
[23] J. Goldberger, R. He, Y. Zhang, S. Lee, H. Yan, H. J. Choi, and P. Yang, Nature (London) **422**, 599 (2003).
[24] H. L. Liu, C. C. Chen, C. T. Chin, C. C. Yeh, C. H. Chen, M. Y. Yu, S. Keller, and S. P. DenBaars, Chem. Phys. Lett. **345**, 245 (2001).
[25] J. Zhang, X. S. Peng, X. S. Wang, Y. W. Wang, and L. D. Zhang, Chem. Phys. Lett. **345**, 372 (2001).
[26] J. Zhang and L. D. Zhang, J. Phys. D **35**, 1981 (2002).
[27] L. Zhang and J. J. Shi, Semicond. Sci. Technol. **20**, 592 (2005).
[28] L. Zhang, J. J. Shi, and T. L. Tansley, Phys. Rev. B **71**, 245324 (2005).
[29] L. Zhang and J. J. Shi, Phys. Status Solidi B **243**, 1775 (2006).
[30] L. Merten, *Atomic Structure and Properties of Solids* (Academic, New York, 1972).
[31] D. E. N. Brancus and E. R. Racec, Rom. J. Phys. **45**, 99 (2000).
[32] C. R. Bennett, N. C. Constantinou, M. Babiker, and B. K. Ridley, J. Phys.: Condens. Matter **7**, 9819 (1995).
[33] A. Gray and G. B. Mathews, *A Treatise on Bessel Functions and Their Applications to Physics* (MacMillan, London, 1922), Chap. VI.
[34] N. Ashkenov *et al.*, J. Appl. Phys. **93**, 126 (2003).
[35] T. Azuhata, T. Sota, K. Suzuki, and S. Nakamura, J. Phys.: Condens. Matter **7**, L129 (1995).
[36] D. E. N. Brancus and E. R. Racec, Balkan Phys. Lett. **7**, 40 (1999).
[37] D. E. N. Brancus and A. C. Mocuta, Can. J. Phys. **73**, 126 (1995).
[38] H.-J. Xie, C. Y. Chen, and B. K. Ma, Phys. Rev. B **61**, 4827 (2000).
[39] L. Wendler and V. G. Grigoryan, Phys. Rev. B **49**, 14531 (1994).
[40] M. Drechsler, D. M. Hofmann, B. K. Meyer, T. Detchprohm, H. Amano, and I. Akasaki, Jpn. J. Appl. Phys., Part 2 **34**, L1178 (1995).
[41] D. E. N. Brancus, G. Stan, and A. Dafinei, J. Phys.: Condens. Matter **17**, 3241 (2005).
[42] J.-J. Shi, X.-Q. Zhu, Z.-X. Liu, S.-H. Pan, and X.-Y. Li, Phys. Rev. B **55**, 4670 (1997).
[43] H. J. Xie, Physica E (Amsterdam) **22**, 906 (2004).
[44] H.-J. Xie and X.-Y. Liu, Superlattices Microstruct. **39**, 489 (2006).